Extended Abstracts of the 2014 International Conference on Solid State Devices and Materials, Tsukuba, 2014, pp98-99

A Comprehensive Modeling of Skin and Proximity Effects for mm-wave Inductors Simulation and Design in Nanoscale CMOS Technology

Jyh-Chyurn Guo and Ren-Jia Chan
Institute of Electronics Engineering, National Chiao Tung University, Hsinchu, Taiwan
Tel: +886-3-5131368, Fax: +886-3-5724361, E-mail: jcguo@mail.nctu.edu.tw

Abstract

A comprehensive model with skin and proximity effects has been developed in this paper to calculate and predict the frequency dependent resistance, $Re(Z_{in})$ and quality factor, Q for mm-wave inductor simulation and design. The derived models incorporate layout and material parameters, and frequency in an explicit form suitable for circuit simulation. The accuracy has been proven by a close match with $Re(Z_{in})$ and Q measured from mm-wave inductor (L_{dc}~150pH, Q_{max}~17, f_{SR}>>65GHz) fabricated by 65nm CMOS process with 0.9μm standard top metal.

I. Introduction

The advancement of CMOS technology to 65nm and beyond can offer ultra-high speed devices with f_T and f_{MAX} boosted to above 300GHz and makes nanoscale CMOS a viable solution for mm-wave design [1]. However, passive devices may become a gating factor in mm-wave circuits. On-Si-chip inductors have been extensively used for impedance matching, LC-tank, filters, and resonators but generally suffer lower quality factor (Q) and narrow bandwidth, due to conductor loss and substrate loss. Skin effect has been known responsible for conductor loss at lower frequency but proximity effect will dominate the conductor loss in a wide bandwidth when approaching mm-wave domain. Furthermore, there is a critical trade-off between skin and proximity effects in inductors design. Proximity effect appears as an important mechanism responsible for an increase of effective resistance and Q degradation in multi-turn spiral inductors [2-3]; however, most of the analysis relies on EM simulation and limited progress is available on analytical models for an efficient and accurate prediction. A first-order analytical model was developed for current crowding effect and approximate formulas were derived for calculating the frequency-dependent resistance **[3]**. However, a number of assumptions and approximation introduced to simplify the formulas leave some open questions. One more critical problem is limited verification by a single set of geometrical parameters for a large inductor with low Q and very narrow bandwidth below 3GHz. Furthermore, skin effect was neglected and led to discrepancy as compared to measurement [3]. The mentioned problems make this first-order analytical model questionable to be applied to mm-wave inductors simulation.

II. Analytical Modeling of Skin and Proximity Effects

First, for analytical modeling of the skin effect, a skin depth δ is defined to calculate the non-uniform current distribution across the metal [4]. The skin depth δ is expressed by (1), in which the higher frequency or the larger σ leads to thinner δ and aggravated skin effect. Taking Cu as an example, its σ =5.531x10^7/Ω-m results in δ as thin as 0.276 μm and 0.214μm at 60 GHz and 100 GHz, which are much thinner than the standard top metal thickness and width in logic CMOS process. Then, the effective thickness t_{eff} can be calculated by integrating the non-uniform current density J due to skin effect and given by (2) in which t is the metal thickness.

$$\delta=\sqrt{2/\omega\mu_0\sigma} \tag{1}$$

$$t_{eff}\left(\omega\right)=\delta(1-e^{-t/\delta}) \tag{2}$$

The frequency dependent resistance due to skin effect, $R_{skin}(\omega)$ can be derived by replacing t with t_{eff}, written as (3)

$$R_{skin}(\omega)=\frac{\ell}{\sigma w\delta(1-e^{-\frac{t}{\delta}})} \tag{3}$$

At very high frequency so that δ<<t, an increase of $R_{skin}(\omega)$, due to skin effect approaches an asymptote as a square root function of ω.

Then, Fig.1 illustrates the basic mechanism underlying the proximity effect. The magnetic field B in an adjacent coil penetrates the target metal trace in the direction normal to the surface. According to Lenz's law, eddy currents will be created in the target metal with a direction to generate a magnetic flux opposite to that introduced from the adjacent coil. As a result, the generated eddy current is added to the excitation current on the inner edge while subtracted from the excitation current on the outer edge. It explains how the proximity effect leads to current crowding and an increase of effective resistance. In the following, an analytical model is derived for calculating the effective resistance associated with eddy currents due to proximity effect, and the introduced excess power loss defined as P_{eddy}.

Fig. 2 shows the eddy current induced in a metal trace due to magnetic fields from the adjacent conducting wires. Assume that the eddy current flows near the edges of the metal only within an effective width of w_{ed}. Applying Ampere's law to Fig.2, the magnetic field B introduced from the neighboring metal wire can be derived as

$$B(i)=\frac{\mu_0 I}{2\pi(w+s)} \tag{5}$$

According to Faraday's law, an electromagnetic field (emf) was generated by the time varying magnetic flux from $B(i)$ in (5) and created an electric field E in a close loop of conductor, given by (6). According to ohm's law and (6), the eddy current can be derived as a function of ωB in (7)

$$\oint_c \vec{E}\cdot d\vec{\ell}=-\frac{d}{dt}\int_s \vec{B}\cdot d\vec{s}\Rightarrow E=\omega Bx \tag{6}$$

$$\vec{J}_{eddy}=\sigma\vec{E}=\sigma\omega Bx \tag{7}$$

This eddy current introduced from adjacent metal wires, due to proximity effect becomes another source of power dissipation and Q degradation in spiral inductors. The power dissipation due to proximity effect induced eddy currents can be calculated as follows. First, specify the eddy currents flow within a finite width of w_{ed} around the edges of a metal trace, as shown in Fig. 2. The local power dissipation P_{eddy}(x) is treated as the joule heating described by (8) associated with the eddy currents I_{eddy} confined in w_{ed} at two edges of the metal trace and resistance R_{eddy}.

$$P_{eddy}(x)=R_{eddy}(x)I_{eddy}^2(x) \tag{8}$$

Then, place $J_{eddy}(x)$ and B given by (7) and (5) into (8) and perform an integration through w_{ed} to achieve an analytical model for the eddy current induced power dissipation expressed by (9)

$$P_{eddy}(i)=\frac{\ell t\sigma\omega^2\mu_0{}^2 I^2}{6\pi^2(w+s)^2}\left[\left(\frac{w}{2}\right)^3-\left(\frac{w}{2}-w_{ed}\right)^3\right] \tag{9}$$

where I is the excitation current in the metal wire. Assume that distribution of eddy current is analogous to that of excitation currents due to skin effect, then w_{ed} can be defined as a skin depth along the width given by (10) and the effective resistance due to eddy current is derived as (11)

$$w_{ed}=\delta(1-e^{-w/\delta}) \tag{10}$$

$$\overline{R_{eddy}}=\frac{\ell t\sigma\omega^2\mu_0{}^2}{6\pi^2(w+s)^2}\left\{\left(\frac{w}{2}\right)^3-\left[\frac{w}{2}-\delta(1-e^{-\frac{w}{\delta}})\right]^3\right\} \tag{11}$$

Then, the total power dissipation P_{ac} and effective resistance R_{ac} under high frequency can be achieved to contain both skin and proximity effects

$$P_{ac} = R_{ac} I^2 = \left(R_{skin} + \overline{R_{eddy}}\right) I^2 \Rightarrow R_{ac} = \left(R_{skin} + \overline{R_{eddy}}\right) \quad (12)$$

Taking (4) and (11) into (12), R_{ac} can be expressed by

$$R_{ac} = \frac{\ell}{\sigma w \delta (1 - e^{-\frac{t}{\delta}})} + \frac{\ell t \sigma \omega^2 \mu_0^2}{6\pi^2 (w+s)^2} \left\{ \left(\frac{w}{2}\right)^3 - \left[\frac{w}{2} - \delta(1 - e^{-\frac{w}{\delta}})\right]^3 \right\} \quad (13)$$

III. Simulation and Measurement Results

Simulation was performed using the derived analytical models to investigate the impact of metal width, space, and thickness on R_{skin}, R_{eddy}, and R_{ac}. First, thick top metal, t=3.35μm and fixed space, S=3μm was specified to verify metal width effect. As shown in Fig.3(a), the wider metal gains the smaller R_{skin} but suffers the larger R_{eddy}.When continuously increasing the width, the increase of R_{eddy} surpasses the decrease of R_{skin} and leads to larger R_{ac} shown in Fig.3(b). The trade-off between skin and proximity effects results in an optimized width, W_{opt} for minimum R_{ac}. W_{opt} is around 3μm for f=30~50GHz and further reduced to 2μm for f≧60GHz (mm-wave regime). It means that the higher frequency leads to the smaller W_{opt}. Fig.4(a) indicates that the wider metal suffers faster increase of R_{ac} when raising frequency. This penalty from proximity effect can be reduced by increasing inter-coil space. Given S=6μm as an example shown in Fig.4(b), the increase of R_{ac} in wider metal can be effectively suppressed by around 35~42% for W≧3μm. Fig.5(a) and (b) present interesting results that metal thickness scaling can effectively reduce R_{ac} in wider metal, attributed to R_{eddy} reduction. The thinner metal to t=2μm and 1μm can cut R_{ac} by around 30~40% and 50~67% in wider metal with W≧3μm. The analytical modeling results provide new insight that thick top metal is no longer necessary for performance and standard top metal with thickness near 1μm can meet the requirement in both aspects like performance and cost.

According to this idea, simulation was performed for mm-wave inductor design using 65nm CMOS with 0.9μm standard top metal and S=2μm to identify the W_{opt} for min. R_{ac}. Fig. 6 indicates that W_{opt} is around 3μm for frequency up to 100GHz. Fig.7(a) illustrates circular inductor fabricated in 65nm CMOS process with top metal t_M=0.9μm and layout given by N=1.5, D_{eff}=21.4μm, W=3μm, and S=2μm to approach target of 150pH for mm-wave design. Fig.7(b) shows the inductance measured up to 65GHz and a close match by simulation. Fig.8(a) and (b) demonstrate $Re(Z_{in})$ and Q determined by $Im(Z_{in})/Re(Z_{in})$ in which f_{SR} is much higher than 65GHz and Q_{max} can reach around 17 for mm-wave design. Furthermore, a good agreement between measurement and simulation proves the accuracy of our developed analytical model.

IV. Conclusion

Our developed analytical models can predict skin and proximity effects, and their trade-off over broadband in mm-wave regime. The simulation results provide a useful guideline that standard top metal with near 1μm thickness and 2~3μm width can meet mm-wave inductor performance at lower cost. The accuracy has been proven by a close match with $Re(Z_{in})$ and Q measured from mm-wave inductor (L_{dc}~150pH, Q_{max}~17, f_{SR}>>65GHz) fabricated by 65nm CMOS process with 0.9μm standard top metal.

Acknowledgement

This work is supported in part by the National Science Council under Grants NSC102-2221-E009-159. Besides, the authors acknowledge the support from NDL for noise measurement and CiC for device fabrication.

References

[1] K.-L. Yeh and J.-C. Guo, *IEEE TED*-60, pp.109-116, 2013.
[2] Y. Cao, *et al.*, *IEEE JSSC*-38, pp.419-426, 2003.
[3] W. B. Kuhn, *et al.*, *IEEE TMTT*-49, pp.31-38, 2001.
[4] H. A. Wheeler, *Proc. IRE*, pp.412-425, 1942.

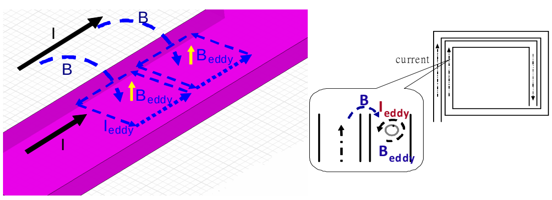

Fig. 1 Eddy currents generated according to Lenz's law, with a direction in/out phase with the excitation current on the inner/outer edges

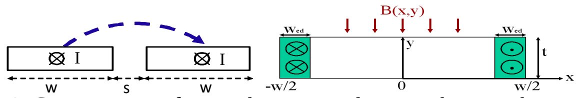

Fig. 2 Cross section of two adjacent metal traces showing the normal magnetic field *B(x,y)*, and eddy current flowing through w_{ed} at two edges.

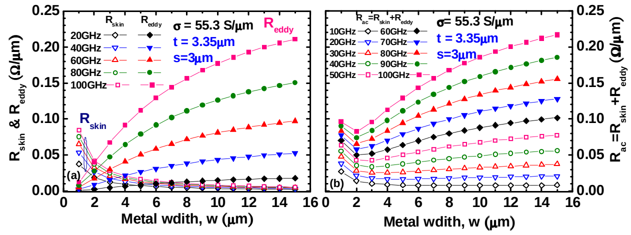

Fig. 3 Simulation by analytical model (a) R_{skin} and R_{eddy} (b) R_{ac}=R_{skin}+R_{eddy} vs. metal width (W=1~15μm), inter-metal space=3μm, thick top metal =3.35μm, f=10~100GHz.

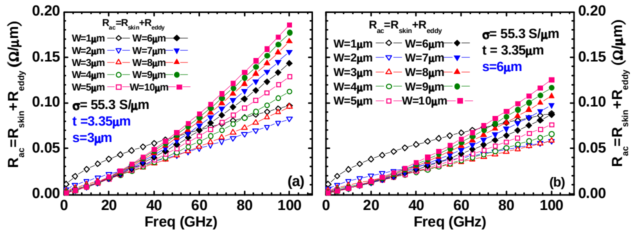

Fig. 4 Simulation by analytical model,R_{ac}=R_{skin}+R_{eddy} vs. freq. (1~100GHz) (a) S=3 μm(b) S=6 μm,W=1~10 μm, thick top metal =3.35 μm.

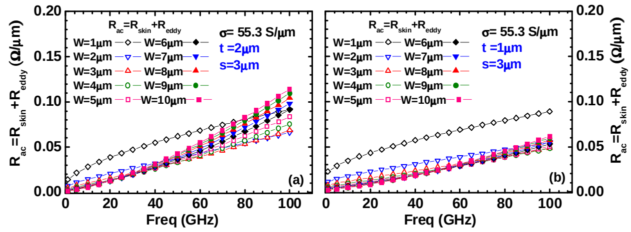

Fig. 5 Simulation by analytical model,R_{ac}=R_{skin}+R_{eddy} vs. freq. (1~100GHz) various metal thicknesses (a) t_M=2 μm(b) t_M=1 μm,W=1~10μm, S =3μm.

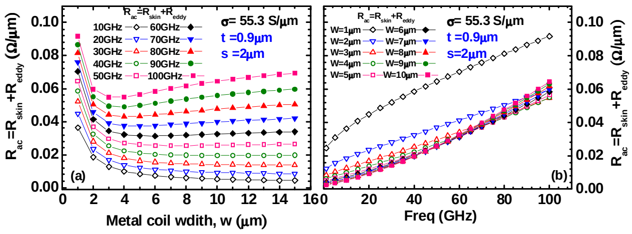

Fig.6 Simulation by analytical model (a),R_{ac} vs. width (10~100GHz) (b) R_{ac} vs. Freq. (W=1~10μm), S=2 μm, standard top metal =0.9μm.

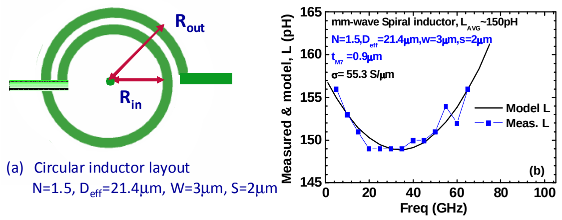

Fig. 7 A mm-wave spiral inductor (a) layout : N=1.5, D_{eff}=21.4μm, W/S/t_{M7}=3/2/0.9μm (b)measured and simulated inductance, L=150~160pH.

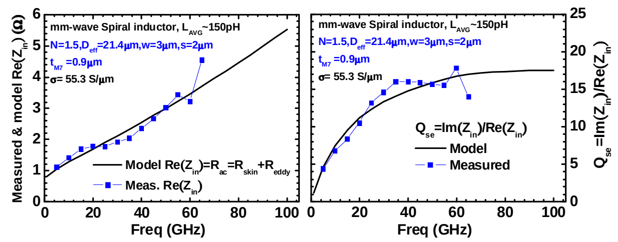

Fig. 8 Measurement and simulation by analytical models (a) $Re(Z_{in})$ (b) $Q_{se}=Im(Z_{in})/Re(Z_{in})$. N=1.5, D_{eff}=21.4μm, W=3μm, S=2μm, t_{M7}=0.9μm.